Contributions, Geophysical Institute, Kyoto University, No. 13, 1973, 21-33

SHORT PERIOD VARIATIONS OF ATMOSPHERIC TEMPERATURE AND ELECTRICAL CODUCTIVITY IN THE STRATOSPHERE

By

Sawako MAEDA, Shun HANDA, Toshio OGAWA, Koji KAWAHIRA and Teruo MIURA*

(Received August 31, 1973)

Abstract

Apparently related fluctuations of atmospheric temperature and electric field and current were simultaneously observed at an approximately constant height level of about 28 km in the stratosphere for about 9 hours at night in a large balloon experiment. The periods of the fluctuations range from about 10 minutes to 2 hours. The phase differences between both variations have roughly equal values between 90° and 180° or −90° and −180° regardless of their periods. Using the polarization factors of temperature and conductivity derived from the theory of atmospheric internal gravity waves, the phase differences are calculated taking vertical wavelength as a parameter, and they are shown to be constant at longer periods than about 20 minutes. It is, however, difficult to explain the large values of the phase differences.

1. Introduction

A comprehensive measurement of electrical elements, i.e., field, current and conductivity in the stratosphere has been made since 1966 by using large balloons. In these measurements short period fluctuations of electrical elements are found often to be related with those of air temperature. The cause of this relation may be either atmospheric waves or the effects of dust or aerosol particles which are concentrated in the temperature inversion layers.

The internal atmospheric gravity waves have become an interesting subject in the upper atmospheric studies since Hines [1960] first suggested that they may be a possible cause in the generation of irregular motions of ionization in the ionosphere. The waves are suggested to be generated in the lower atmosphere, and they propagate into the upper atmosphere. Pittwey and Hines [1963], Hines [1965], and Hines and Reddy [1967] discussed dissipation of these waves by viscous damping and thermal conduction during the propagation to the upper atmosphere. There are, however, very few works on direct measurement of the gravity waves in the stratosphere.

The aircraft measurement is an effective means to observe gravity waves, by which Axford [1970, 1971] reported on gravity waves in shear flow at the height of 12.6 km showing the potential temperature variations of up to ±2° C. Beyers and

* Faculty of Science, Osaka City University, Osaka.

Miers [1970] observed that wavelength and amplitude of wave-like trajectory of the zero-pressure balloon in the stratopause region were similar to those of mountain waves in the troposphere.

In this paper we report on the apparently related fluctuations of temperature and electrical conductivity simultaneously observed by a large balloon at an approximately constant height level in the stratosphere, and compare the result with the theory of atmospheric internal gravity waves. The other possibility of the cause of this phenomenon, i.e., the effect of particulate material concentrations, is not surveyed in this paper.

2. Observation

In 1971 a balloon experiment was conducted on 7 through 8 October, at the Sanriku Balloon Center, Institute of Space and Aeronautical Science, University of Tokyo (39°09′30″N, 141°49′30″E; about 100 km north of Sendai). A large plastic balloon of a volume of 5000 m³ was launched at 16:43 JST on 7 October. After 98 minutes from the launching it reached the height of 27.8 km. The average ascending rate was 4.8 m/sec. The balloon then made a level flight at an approximately constant altitude. The balloon flew over the Pacific Ocean from Sanriku to a distance about 585 km ENE during 24 hours after the launching. The balloon trajectory is shonw in Fig. 1.

The air temperature was measured with a bead-type thermister sensor of 1.5 mm in diameter and 3 mm in length. Accuracy of the temperature measurement was

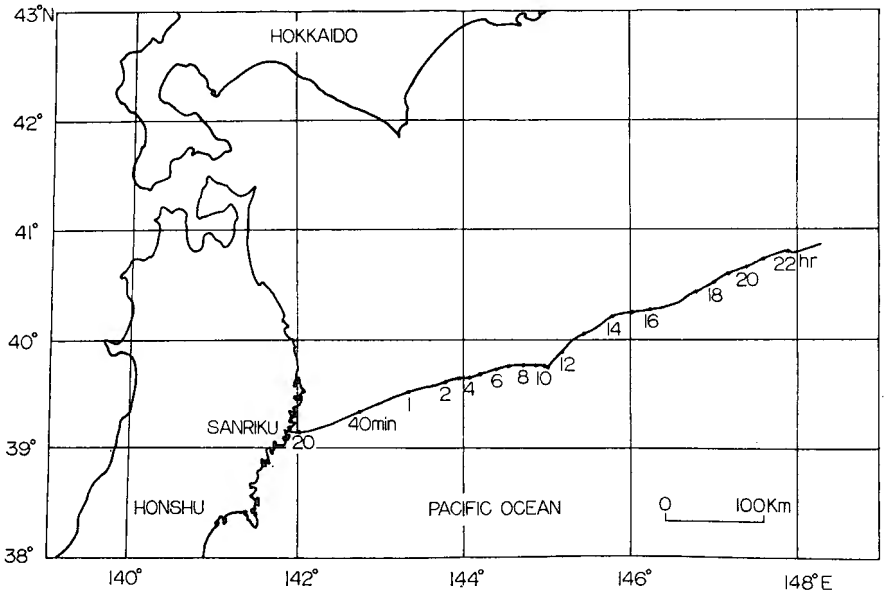

Fig. 1. Balloon trajectory. Flight times are indicated.

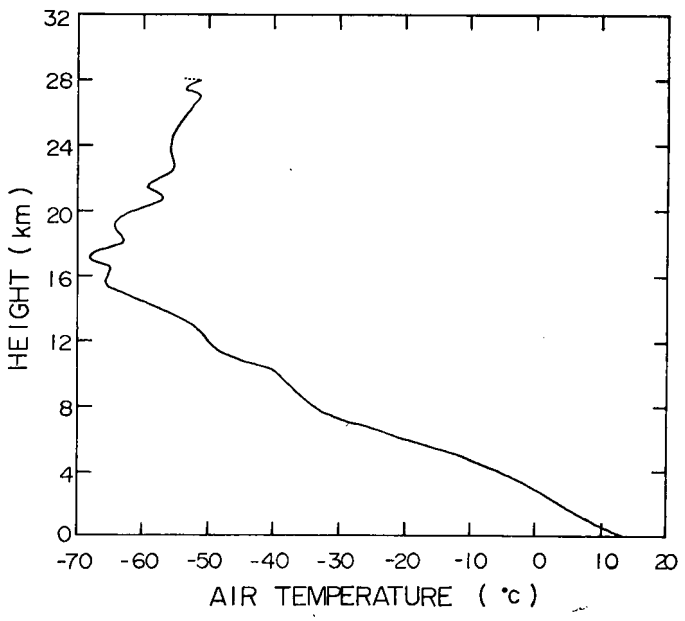

Fig. 2. Vertical profile of air temperature at 1643 JST on 7 October 1971.

$\pm 0.2°$. The vertical profile of the temperature is shown in Fig. 2.

The vertical electric field and current were measured with an antenna consisting of a pair of steel wires of 2 mm in diameter and 10 m in length, which was suspended about 90 m below the balloon in order to keep it out of any effect of electric charge on the balloon. Measurement accuracies of the electric field and the current were ± 3 mV/m and $\pm 3 \times 10^{-14}$ A/m^2 respectively. Details of instrumentation are described by Ogawa et al. [1970].

3. Synoptic Situation

A cold front was lying from NE to SW along the Japan Islands at a distance of several hundreds of kilometers east of Sanriku. A simplified ground weather map at 21h JST on 7 October is given in Fig. 3a. A 500 mb equi-pressure contours at the same time is given in Fig. 3b. In this figure is shown the region of maximum wind speed of 31 m/sec, which might be the bottom of the jet stream lying to the west of the cold front.

From the analysis of the balloon trajectory, the horizontal wind velocity was obtained and is shown in Fig. 4, in which the vertical profile can roughly be seen. It is recognized that the jet stream has the maximum wind speed of 76 m/sec at the altitude of 12 km. At the balloon floating level of about 28 km, approximately eastward wind speed is about 6 m/sec.

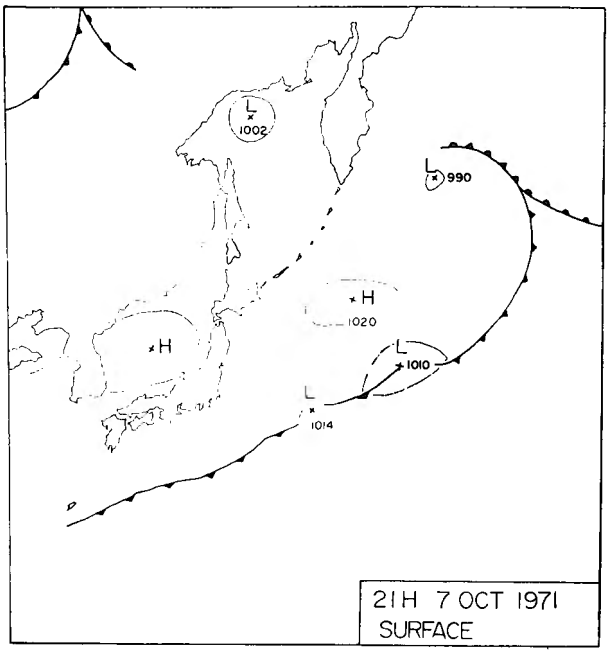

Fig. 3a. Simplified weather map at 21 h JST on 7 October 1971. Surface pressure in mb. A cold front was lying from NE to SW along the Japan Islands at a distance of several hundreds of kilometers east of Sanriku.

As can be seen in Fig. 2 the temperature decreased from the ground value down to −68 °C at 17 km height, then increased up to −51 °C at the balloon floating level in the stratosphere. It can also be seen in Fig. 2 that the vertical temperature gradient is about 1.3 °K/km near the floating altitude, and the vertical temperature profile is accompanied by fluctuations of about ± 2 °K from the background.

In order to see stability of a shear layer in the background atmosphere, the Richardson number ($R_i=(g/\theta)(\partial\theta/\partial z)/(\partial U/\partial z)^2$) was calculated from the wind speed (U) and temperature (T) profiles, where g is the gravitational acceleration, θ is potential temperature, and z is taken upward in the Cartesian co-ordinate. The vertical profile of the Richardson number thus calculated is shown in Fig. 5. Fig. 5 shows that the Richardson number for the layer above 8 km is greater than 1.0, implying a region of stable air flow, while the Richardson number is 0.3 in the layer between 6 and 8 km. This layer has a possibility of generation of turburence in it, since the Richardson number is close to $R_i \leqq 1/4$ which is generally considered a critical value for onset of wave instability in a shear flow (Miles and Howard [1964]).

4. Observational Results

Time variations of the air temperature (T), the vertical electric field (E) and

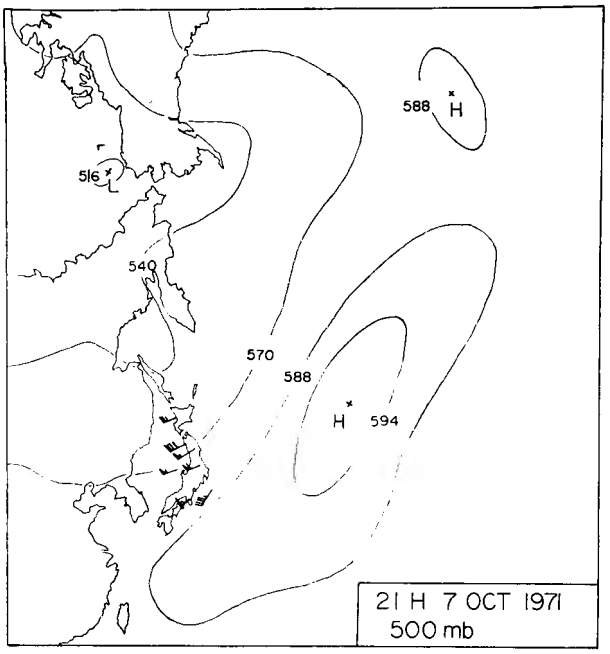

Fig. 3b. 500 mb equi-pressure contours at the same time in Fig. 3a and a region of maximum wind speed of 31 m/sec (60 knot) above the Japan Island, which might be the bottom of jet stream lying to the west of the cold front (500 mb contours in decameters).

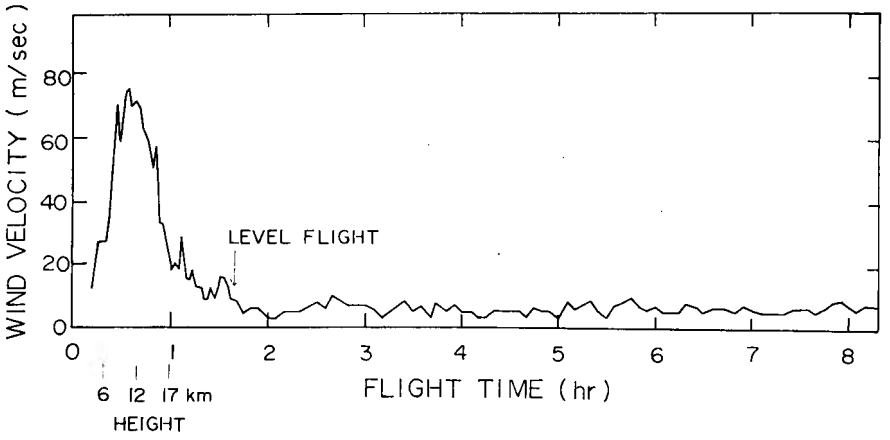

Fig. 4. Horizontal wind velocity obtained from the analysis of the balloon trajectory. It is recognized that the jet stream has the maximum wind speed of 76 m/sec at the altitude 12 km.

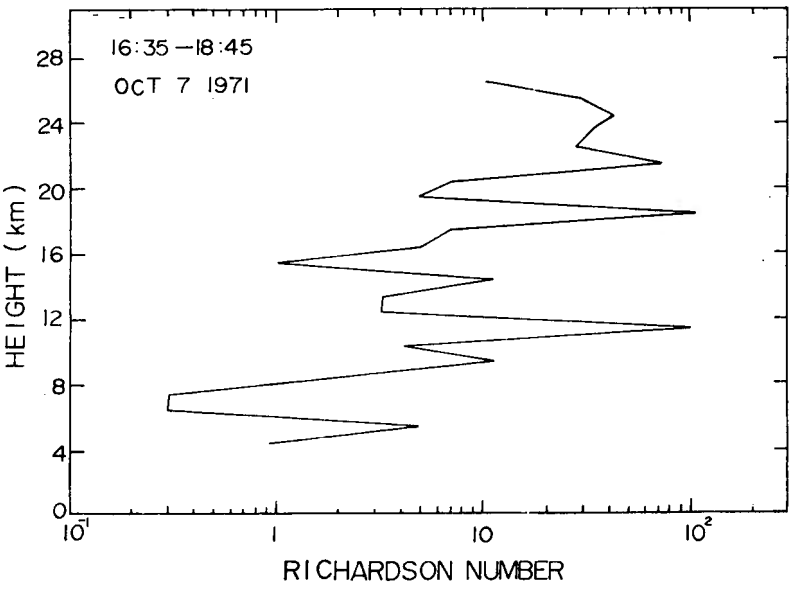

Fig. 5. Vertical profile of Richardson number at 1635–1845 JST 7 October. Richardson number is 0.3 in the layer between 6 and 8 km, which implies that this layer has a possibility of generation of turbulence.

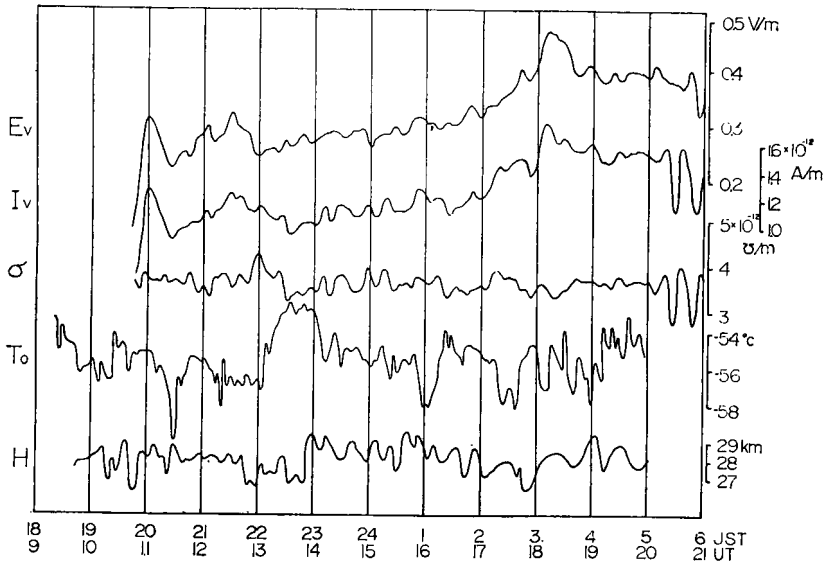

Fig. 6. Time variations of vertical electric field (E), current (I), conductivity (σ), air temperature (T) and balloon height (H). Electrical conductivity was calculated from Ohm's law ($\sigma = I/E$). Balloon height (H) was tracked by radar sounding.

current (I) are shown in Fig. 6, where only data for night time are used because the temperature sensor did not work properly, being affected by the solar radiation after the sunrise on 8 October. The electrical conductivity (σ) was calculated assuming Ohm's law ($\sigma=I/E$) to be valid in a quasi-stationary state. Time variations of σ thus obtained are also shown in Fig. 6. Data were originally received on the telemeter every 3–4 minutes for T and 6–8 minutes for E and I according to the time lapsed, but the final digital data were read every 3 minutes from the smoothed curves reproduced on a graph paper.

The mean value of the temperature is 219.6 °K (−53.4 °C) and the amplitude of its fluctuations is about ±2 °K, approximately corresponding to the balloon vertical-

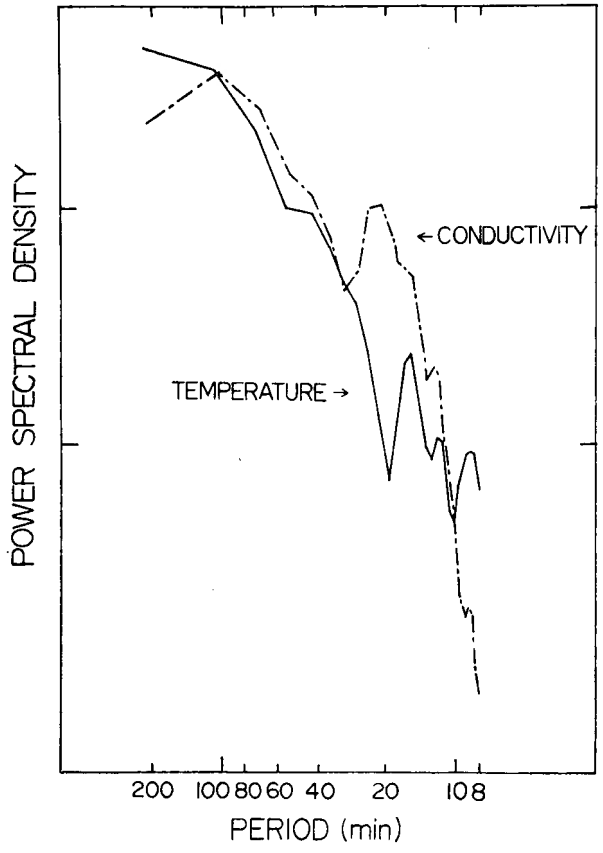

Fig. 7. Power spectra of temperature and conductivity variations. There is a plateau of the power at the period of 100–200 minutes in the spectrum of temperature, while there is a peak at the period of 100 minutes in the spectrum of conductivity. There is a sharp decreasing at about 20 minutes in the temperature, while an enhanced power can be seen at about the same period in the conductivity.

motion of about ± 1.5 km. Periods of fluctuations range from about 10 to 120 minutes. The mean value of the electrical conductivity is 3.6×10^{-12} $\mho$/m and the amplitude of its fluctuations is about $\pm 10\%$ of its mean value, approximately corresponding to the balloon vertical-motion of about ± 0.8 km considering a proper vertical profile of the conductivity. The balloon height tracked by radar sounding is also plotted for reference in Fig. 6. The angle of elevation of the balloon is less than about 8° after 2 hours from launching, so that the height observation is not very accurate. It, however, gives some idea of the balloon vertical-motion.

The power spectra of the temperature and conductivity variations were calculated and are shown in Fig. 7. There is a plateau of the power at the period of 100–200 minutes in the spectrum of temperature, while there is a peak at the period of 100 minutes in the spectrum of conductivity. In shorter period region there is a sharp decreasing at about 20 minutes in the temperature, while an enhanced power can be seen at about the same period in the conductivity. Except for this period region, however, it may be said that the spectral shapes of both the temperature and the conductivity are similar to each other

The inverse correlation between temperature and conductivity variations is clear in Fig. 6. Cross-correlation between both variations also shows the inverse correlation, the coefficient being -0.4 at the time lag 0. In order to see the phase relation of the temperature and conductivity variations in more detail, phase differences between

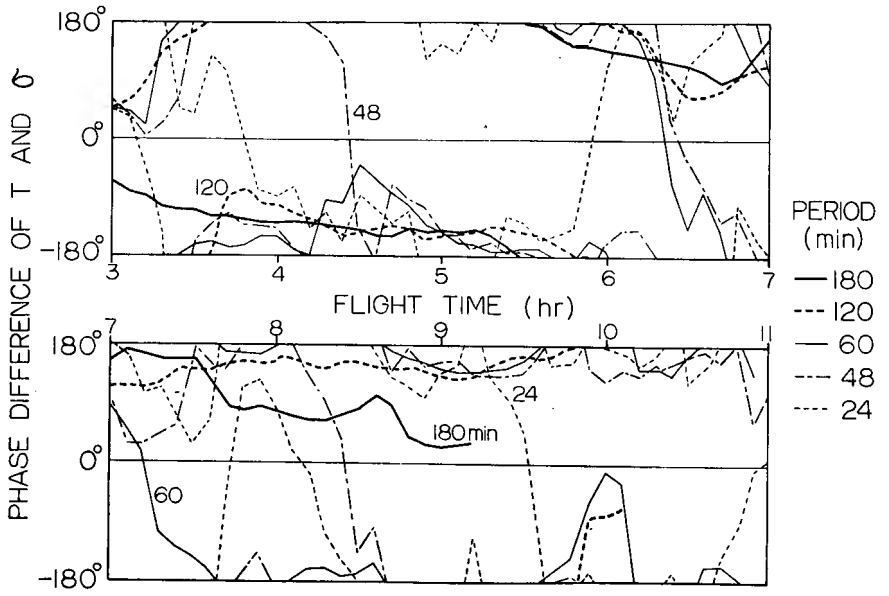

Fig. 8. Phase differences between both the same frequency components of temperature and conductivity. They are estimated from the ratios of Fourier cosine and sine coefficients of the variations. It is evident that the phase differences are roughly equal values between 90° and 180° or $-90°$ and $-180°$ for all the Fourier components.

both the same frequency components were estimated from the ratios of Fourier cosine and sine coefficients of the variations. The result is shown in Fig. 8 for the periods of 180, 120, 60, 48, and 24 minutes. It is seen in Fig. 8 that the phase differences have roughly equal values between 90° and 180° or −90° and −180° for all the Fourier components throughout the balloon flight time.

5. Discussion

The observational results described above may suggest the existence of any dynamical motions of the atmosphere in the periods of 10–120 minutes which are the same periods as have the internal gravity waves (Gossard [1962]). The meteorological situation also suggests a possibility of generation of such waves (Hines [1968]).

The power spectrum of the internal gravity waves has a 'cut-off' at the resonance frequency ($=\omega_B \cos\theta$; ω_B is the Brunt-Väisälä frequency given later and θ is the angle between the wave number vector and the horizontal axis) (Hines [1960], Gossard [1962]). The 'cut-off' period changes with the value of θ or by the Doppler shift due to the background mean flow. If the wave field is isotropic, its spectrum has the 'cut-off' period; $\tau_B=2\pi/\omega_B$. As the Brunt-Väisälä period τ_B at the height of 28 km is about 5 minutes, the sharp decreasing at about 20 minutes in the spectrum of temperature in Fig. 7 may correspond to this 'cut-off' period in the internal gravity waves.

The electrical conductivity in the atmosphere is discussed by Israël [1957]. If the ionization equilibrium exists, the electrical conductivity due to small ions in the stratosphere may be represented by the equation

$$\sigma=2nek\simeq 2(q/\alpha)^{1/2}ek, \tag{1}$$

where n is number density of ions both positive and negative, e is elementary charge, k is electrical mobility which is in inverse proportion to the atmospheric density, q is production rate of ions, which is proportional to the atmospheric density, provided that cosmic rays are only one ionization source, and α is the recombination coefficient. Then

$$k=k_{oo}(p_{oo}/p)(T/T_{oo}), \tag{2}$$

$$q=q_{oo}(p/p_{oo})(T_{oo}/T), \tag{3}$$

where suffix oo represents quantity in the standard atmosphere and p is atmospheric pressure. The recombination coefficient may be written as

$$\alpha=\alpha_{oo}(p/p_{oo})(T_{oo}/T)^{7/3}. \tag{4}$$

Substituting Eqs.(2), (3) and (4) into Eq.(1), the conductivity may be written as

$$\sigma=\sigma_{oo}(p_{oo}/p)(T/T_{oo})^{5/3}. \tag{5}$$

On the assumption that the density is constant,

$$p_{oo}/p = T_{oo}/T. \tag{6}$$

From Eqs.(5) and (6)

$$\sigma = \sigma_{oo}(T/T_{oo})^{2/3}. \tag{7}$$

Equation (7) implies that the conductivity varies with the temperature in phase. Consequently, for the explanation of phase difference between σ and T observed in the present experiment, there needs an introduction of any atmospheric motion which causes a density change.

The essential characteristics of internal gravity waves in the isothermal atmosphere were developed by Hines [1960]. According to his theory, a Fourier component of each parameter of the neutral atmosphere is represented with the polarization factors P and Q as

$$p'/p_oP = \rho'/\rho_oQ = A\exp(\gamma gz/2c^2)\times\exp i(\omega t - k_x x - k_z z), \tag{8}$$

where p' and ρ' are perturbed quantities of pressure and density, p_o and ρ_o are unperturbed pressure and density, A is a constant presumed small, γ is the ratio of specific heat, c is the sound velocity, ω is the real angular frequency of the wave, and k_x and k_z are the corresponding real wave numbers, x being a horizontal Cartesian co-ordinate measured in any direction perpendicular to z-axis. The wave numbers k_x and k_z are related to the wave frequency ω by the dispersion equation;

$$\omega^4 - \omega^2c^2(k_x^2+k_z^2) + (\gamma-1)g^2k_x^2 - \gamma^2g^2\omega^2/4c^2 = 0. \tag{9}$$

The polarization factors P and Q can be written as

$$P = \gamma\omega^2[k_z - i(1-\gamma/2)g/c^2], \tag{10}$$

$$Q = \omega^2k_z + i(\gamma-1)gk_x^2 - i\gamma g\omega^2/2c^2, \tag{11}$$

which determine the relative phases of the pressure and density variations.

Similarly if the temperature and electrical conductivity are affected by the gravity waves, the polarization factors of temperature and conductivity T and $\sum$ may be expressed as

$$T'/T_oT = \sigma'/\sigma_o\sum = A\exp(\gamma gz/2c^2)\times\exp i(\omega t - k_x x - k_z z), \tag{12}$$

where T' and σ' are perturbed quantities of temperature and conductivity, and T_o and σ_o are unperturbed temperature and conductivity. Using the equation of state of the ideal gas; $p_o+p' = (\rho_o+\rho')R(T_o+T')$,

$$\frac{T'}{T_o} = \frac{p'}{p_o} - \frac{\rho'}{\rho_o}, \tag{13}$$

where R is the ideal gas constant. Similarly as Eq.(5) can be rewritten as

$$\sigma = \sigma_o(p_o/p)(T/T_o)^{5/3}, \tag{14}$$

$$\sigma_o+\sigma' \simeq \sigma_o\left(1-\frac{p'}{p_o}+\frac{5}{3}\frac{T'}{T_o}\right). \tag{15}$$

From Eq.(15)

$$\frac{\sigma'}{\sigma_o}=\frac{5}{3}\frac{T'}{T_o}-\frac{p'}{p_o}. \tag{16}$$

Then the polarization factors T and $\sum$ can be derived from Eqs.(10), (11), (12), (13) and (16) as

$$T=P-Q=\omega^2 k_z(\gamma-1)+i(\gamma-1)g(\gamma\omega^2/2c^2-k_x^2), \tag{17}$$

$$\sum=\frac{5}{3}(P-Q)-P=\left(2\gamma/3-\frac{5}{3}\right)\omega^2 k_z+i\left[\gamma g\omega^2/3c^2\left(\gamma+\frac{1}{2}\right)-\frac{5}{3}(\gamma-1)gk_x^2\right]. \tag{18}$$

The phase difference between the temperature and the conductivity $\Delta\phi$ can be calculated from the real and imaginary parts of the complex quantities T and $\sum$ as

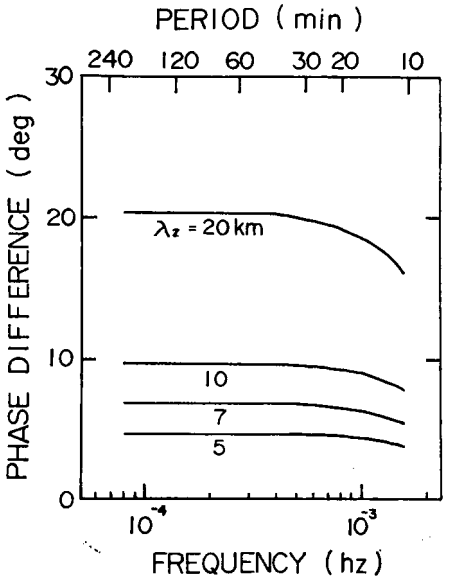

Fig. 9. Theoretical result of phase differences between temperature and conductivity taking vertical wave length λ_z as a parameter. The basic parameters adopted in the calculation are $\gamma=1.4$, $g=9.8$ m/sec^2 and $c=280$ m/sec. Phase differences are almost constant regardless of wave periods at the longer periods than about 20 minutes, but the magnitudes of phase differences are relatively small.

$$\Delta\phi=\tan^{-1}[\mathrm{Im}(T)/\mathrm{Re}(T)]-\tan^{-1}[\mathrm{Im}(\sum)/\mathrm{Re}(\sum)]. \tag{19}$$

The result of this calculation taking vertical wave length λ_z as a parameter is shown in Fig. 9. The basic parameters adopted in the calculation are $\gamma=1.4$, $g=9.8$ m/sec^2, $c=280$ m/sec. The phase differences are about 4.6°, 6.7°, 9.6° and 20.3° for the assumed vertical wave lengths of 5 km, 7 km, 10 km and 20 km respectively. The phase differences are almost constant regardless of wave periods at the longer periods than about 20 minutes.

The dispersion equation (9) becomes simple at such a low frequency that $\omega \ll \omega_B$;

$$\omega^2 k_z^2 \simeq \omega_B^2 k_x^2, \tag{20}$$

where ω_B is the Brunt-Väisälä frequency in the isothermal atmosphere and is given by

$$\omega_B^2=(\gamma-1)g^2/c^2. \tag{21}$$

In this circumstance $\Delta\phi$ to be determined by Eq. (19) depends only on k_z and is independent on the frequency ω. As the frequency ω increases toward ω_B, $\Delta\phi$ becomes to depend on ω, as can be seen in Fig. 9. The experimental result that the phase difference between the temperature and the conductivity is roughly constant regardless of the periods may be explained by the above theoretical result on the internal gravity waves, but the magnitudes of phase differences cannot be explained by the present consideration.

The above described discussion does not bring any conclusion in seeing whether or not the observed fluctuations of air temperature and electrical conductivity are caused by the atmospheric internal gravity waves. Nevertheless the observed phenomena are very interesting and exciting, and it is the purpose of this paper to contribute to atmospheric physics by mainly presenting the new observed facts.

In future work a multi-balloon measurement separated about 100 km, for example, from each other is highly desirable to see the spacial extent and/or propagation velocity of the phenomena.

Acknowledgement

This work is one of the results in a series of large balloon experiments to measure electric fields and currents in the stratosphere. The authors thank Professors J. Nishimura and H. Hirosawa and the other members at the Sanriku Balloon Center, Institute of Space and Aeronautical Science, University of Tokyo for their great help in the balloon launching and data telemetering.

References

Axford, D. N., 1970; An observation of gravity waves in shear flow in the lower stratosphere, Quart. J. R. Met. Soc., **96**, 273–286.

Axford, D. N., 1971; Spectral analysis of an aircraft observation of gravity waves, Quart. J. R. Met. Soc., **97**, 313–321.

Beyers, N. J. and B. T. Miers, 1970; Measurements from a zero-pressure balloon in the stratopause (48 km), J. Geophys. Res., **75**, 3513–3522.

Gossard, E. E., 1962; Vertical flux of energy into the lower ionosphere from internal gravity waves generated in the troposphere, J. Geophys. Res., **67**, 745–757.

Gossard, E. E., J. H. Richter and D. Atlas, 1970; Internal waves in the atmosphere from high-resolution radar measurements, J. Geophys. Res., **75**, 3523–3536.

Hicks, J. J., 1969; Radar observations of a gravitational wave in clear air near the tropopause associated with CAT, J. Appl. Met., **8**, 627–633.

Hines, C. O., 1960; Internal atmospheric gravity waves at ionospheric heights, Can. J. Phys., **38**, 1441–1481.

Hines, C. O., 1965; Dynamical heating of the upper atmosphere, J. Geophys. Res., **70**, 177–183.

Hines, C. O., 1968; A possible source of waves in noctilucent clouds, J. Atmosph. Sci., **25**, 937–942.

Hines, C. O. and C. A. Reddy, 1967; On the propagation of atmospheric gravity waves through regions of wind shear, J. Geophys. Res., **72**, 1015–1034.

Israël, H., 1957; *Atmosphärische Elektrizität*, Teil I, Akademische Verlags, Leipzig, 370 pp.

Miles, J. W. and L. N. Howard, 1964; Note on a heterogeneous shear flow, J. Fluid Mech., **20**, part 2, 331–336.

Ogawa, T., Y. Tanaka and K. Tanaka, 1970; Measurement of three components of electric fields and currents in the stratosphere, Large Balloon Symposium, Inst. of Space and Aeronautical Sci., Univ. of Tokyo, 34–48. (in Japanese)

Pittewey, M. L. V. and C. O. Hines, 1963; The viscous damping of atmospheric gravity waves, Can. J. Phys., **41**, 1935–1948.